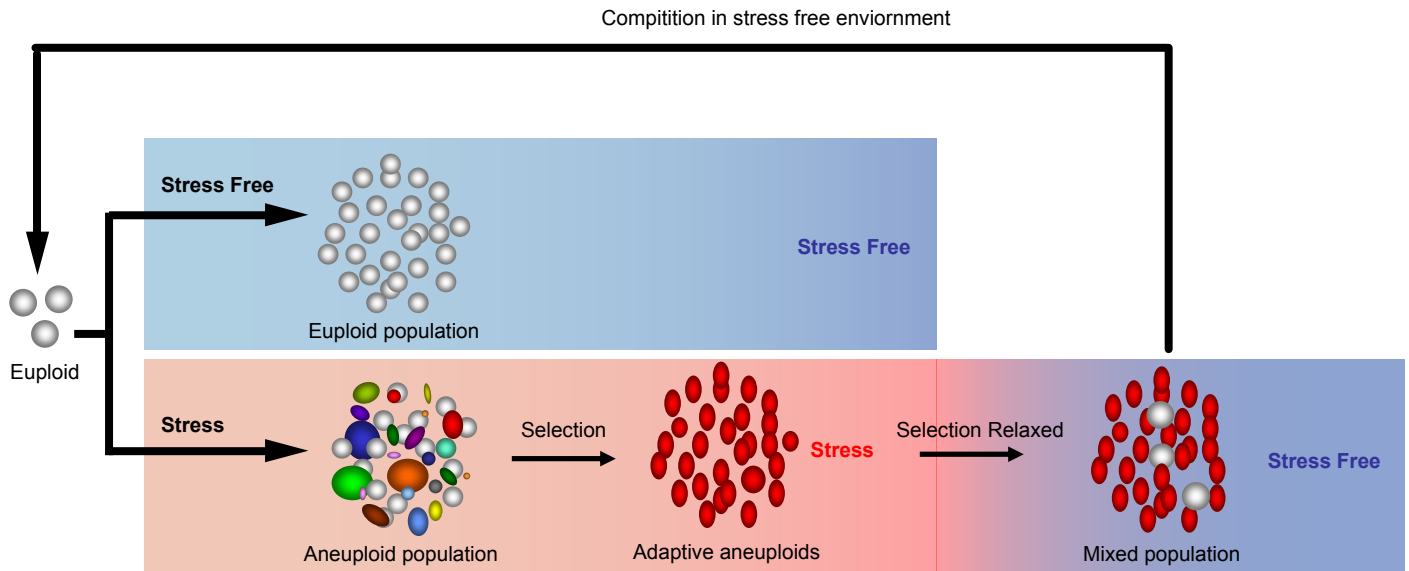
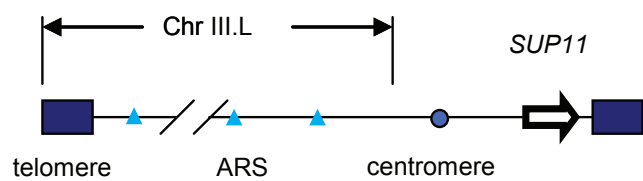


# Supplementary Figure 1



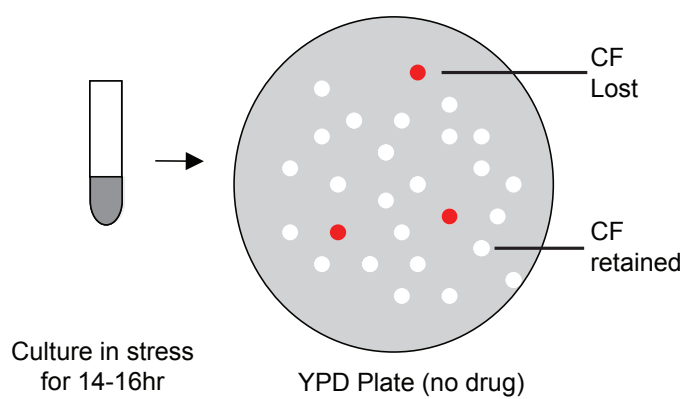
# Supplementary Figure 2

**a**



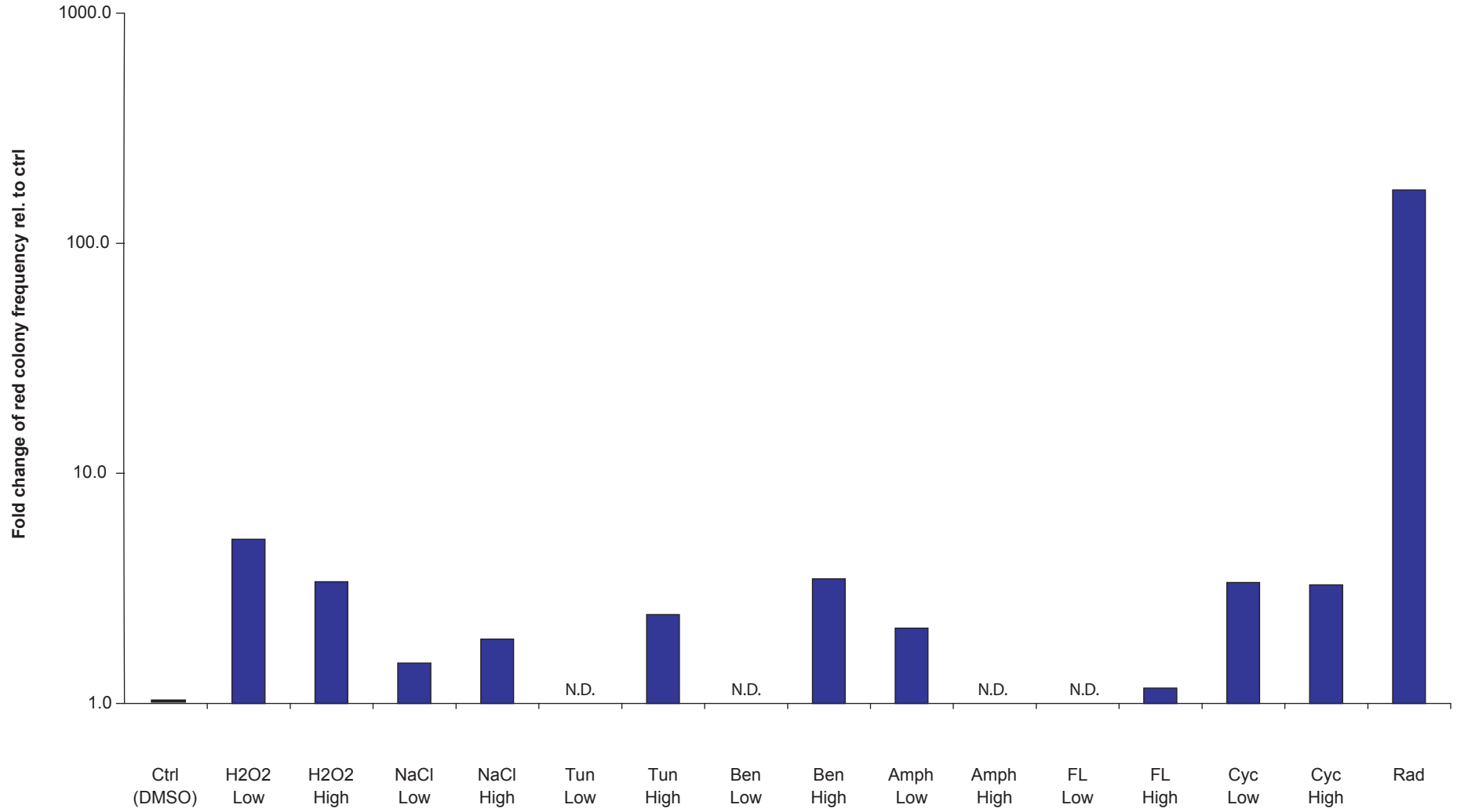
**Structure of the artificial chromosome**

**b**

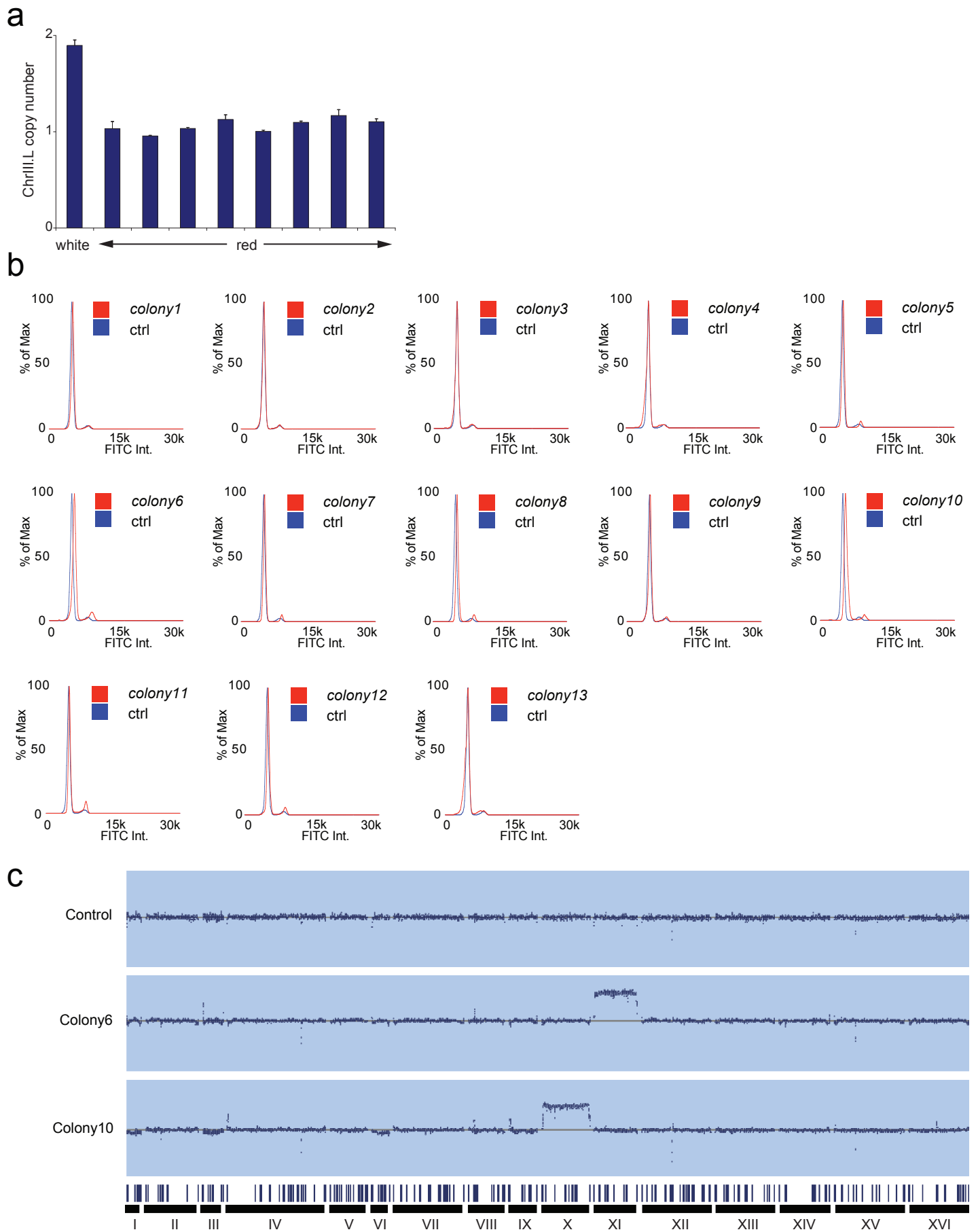


# Supplementary Figure 3

Name	Ctrl (DMSO)	H <sub>2</sub> O <sub>2</sub> Low	H <sub>2</sub> O <sub>2</sub> High	NaCl Low	NaCl High	Tun Low	Tun High	Ben Low	Ben High	Amph Low	Amph High	FL Low	FL High	Cyc Low	Cyc High	Rad Low
Concentration (w/v or v/v)	1%			37.5g/L	75g/L	5µg/ml	10µg/ml	30µg/ml	60µg/ml	0.4µg/ml	0.8µg/ml	100µg/ml	200µg/ml	0.5µg/ml	1µg/ml	10µg/ml
Concentration (in molar)		1.125mM	2.25mM	0.65M	1.3M	6µM	12µM	104µM	208µM	430nM	860nM	327µM	654µM	2µM	4µM	27µM
Total Colonies	40752	3875	1614	3038	1435	628	1868	2955	2874	3423	2685	1898	1560	1355	2780	592
Red Colonies	47	22	6	5	3	0	5	1	11	8	3	1	2	5	10	111
Red Colony Frequency (1x10 <sup>3</sup> )	1.1	5.7	3.7	1.6	2.1	0.0	2.7	0.3	3.8	2.3	1.1	0.5	1.3	3.7	3.6	187.5
OD <sub>final</sub>	7.0	0.7	0.4	5.3	0.6	1.1	0.6	4.3	0.7	4.5	0.5	2.3	2.4	1.1	0.5	6.5
Number of Cell Cycles	5.1	1.8	1.0	4.7	1.6	2.5	1.6	4.4	1.8	4.5	1.2	3.5	3.6	2.5	1.4	5.0
Chr. Loss Rate (1x10 <sup>-3</sup> /division)	0.2	5.6	6.5	0.4	1.8	N.D.	2.5	N.D.	3.6	0.8	0.9	N.D.	0.4	2.5	4.2	74.4

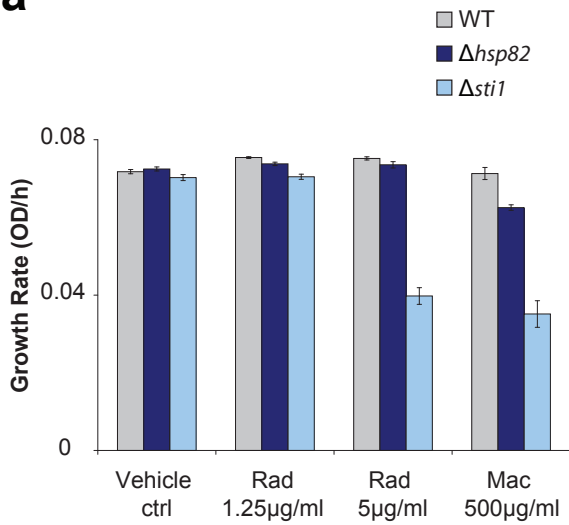


# Supplementary Figure 4

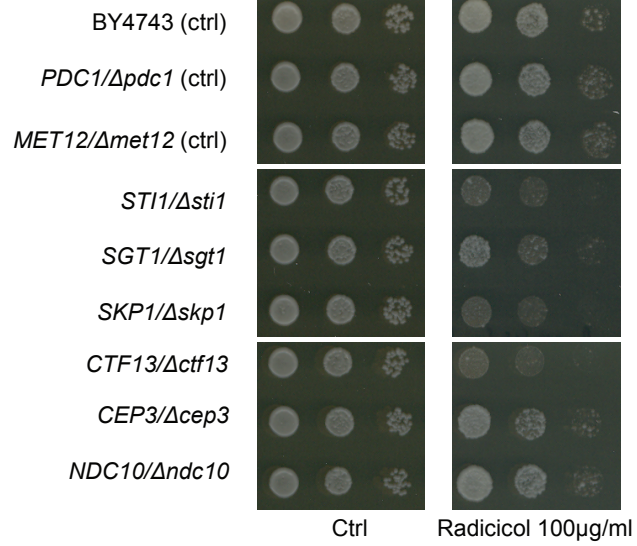


# Supplementary Figure 5

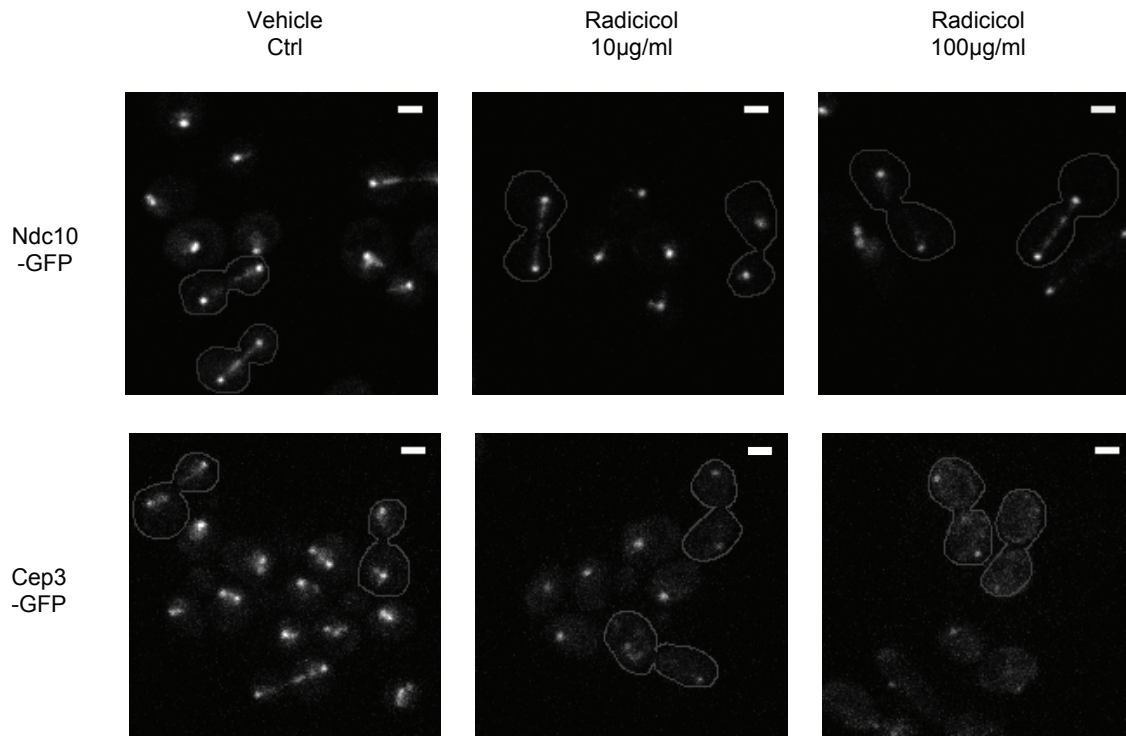
**a**



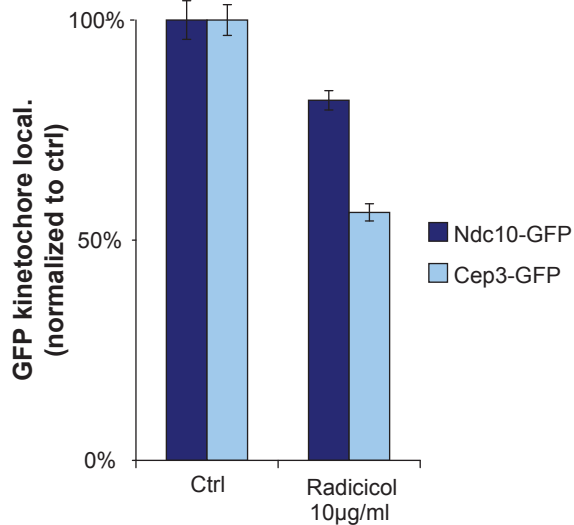
**b**



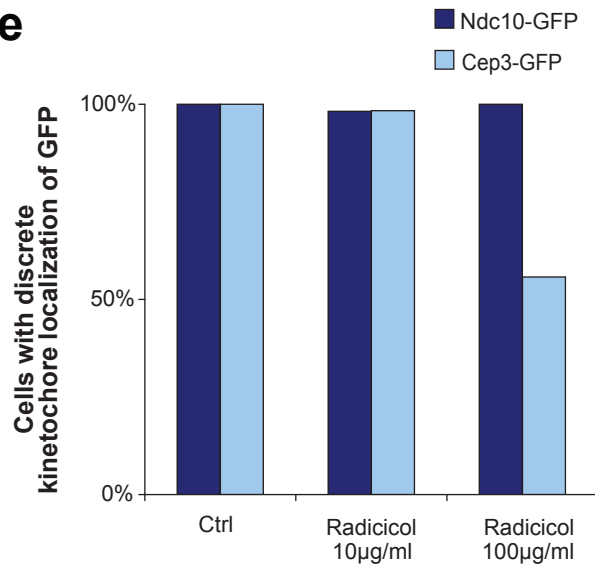
**c**



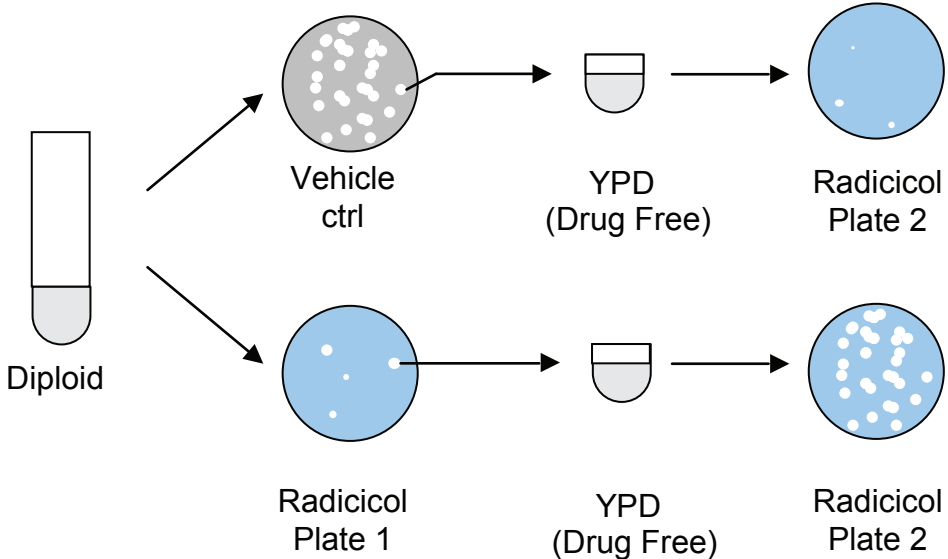
**d**



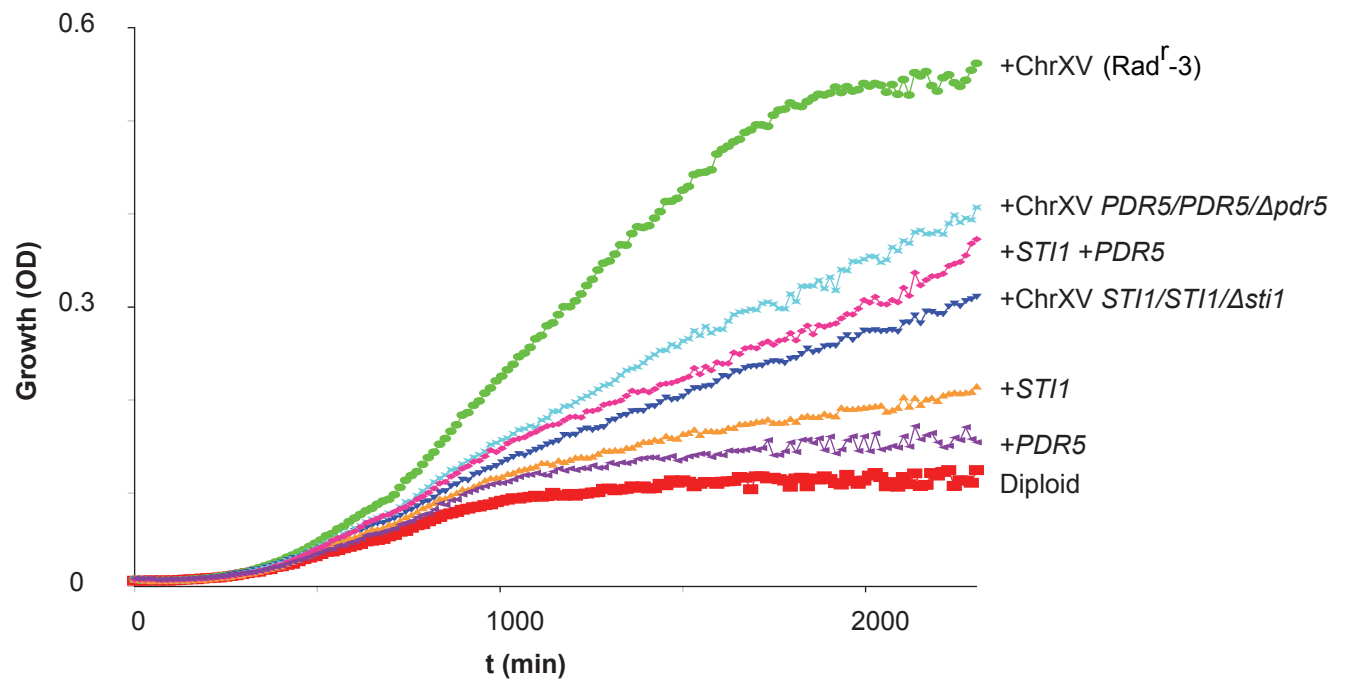
**e**



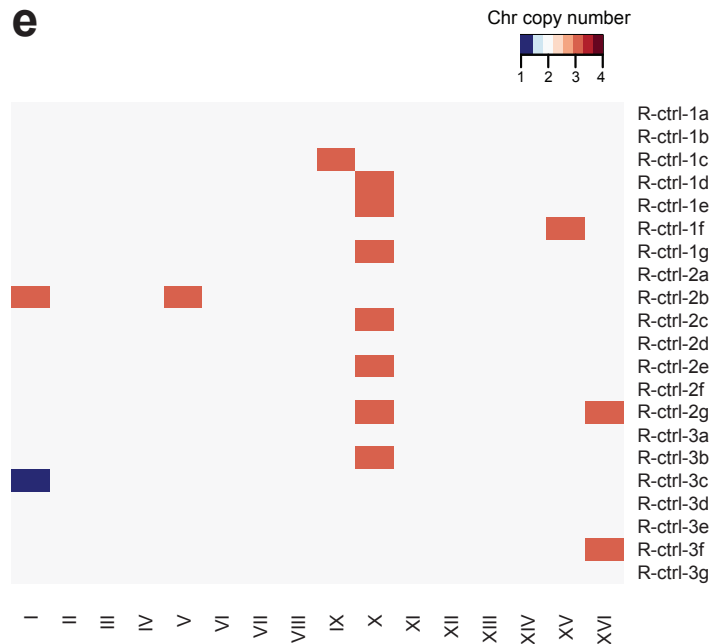
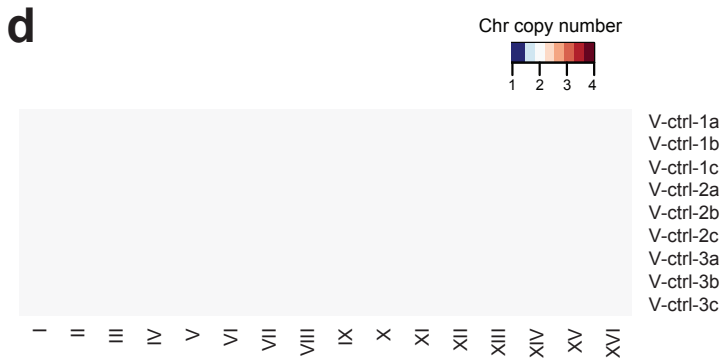
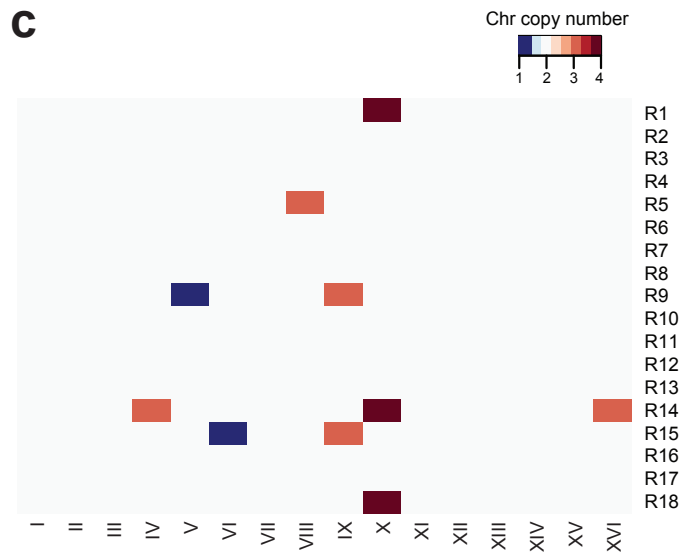
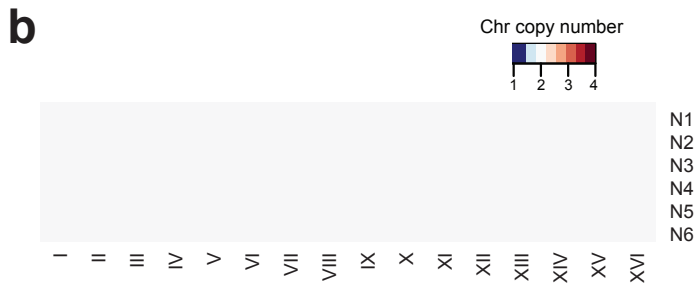
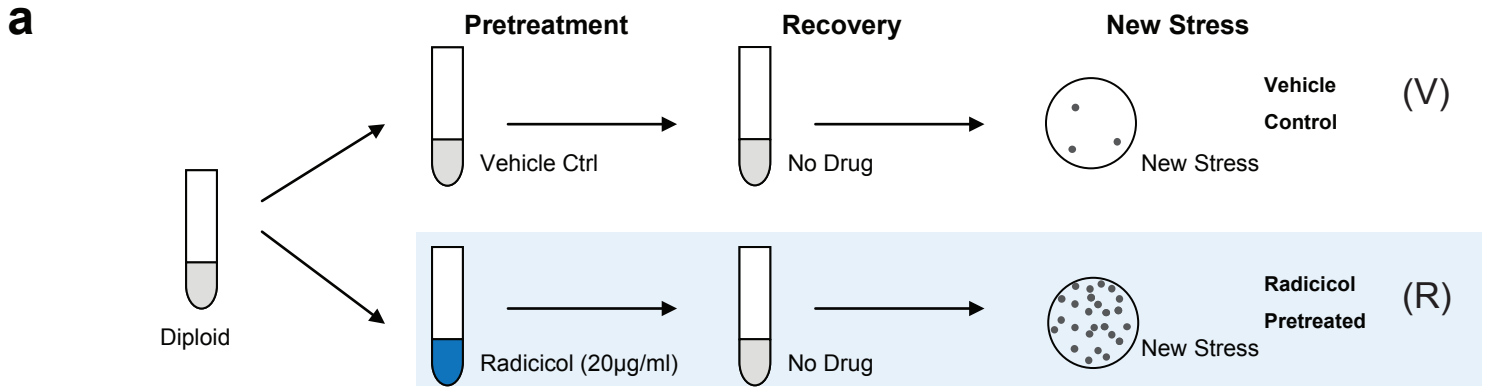
# Supplementary Figure 6



Supplementary Figure 7



# Supplementary Figure 8

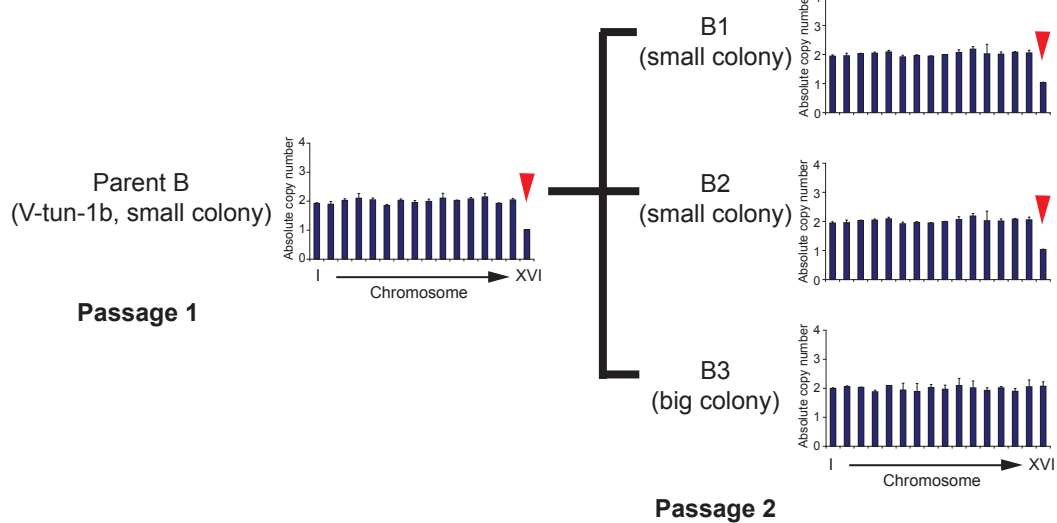




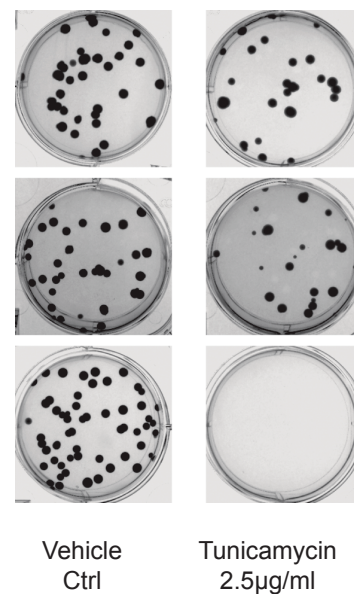


# Supplementary Figure 10

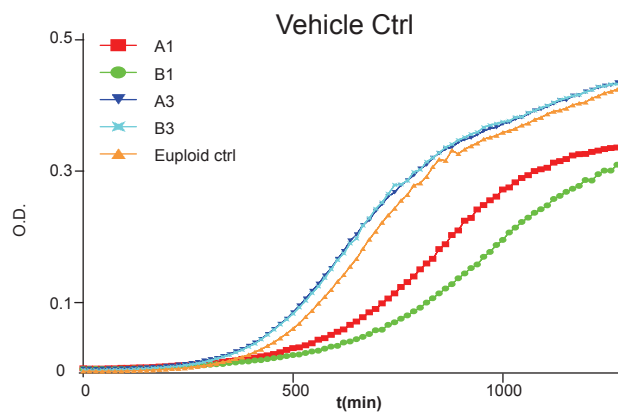
**a**



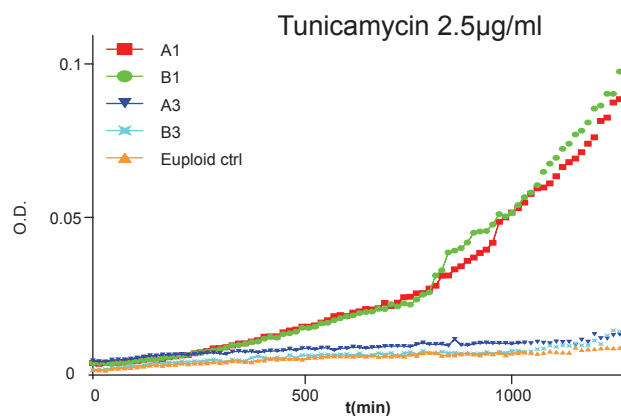
**b**



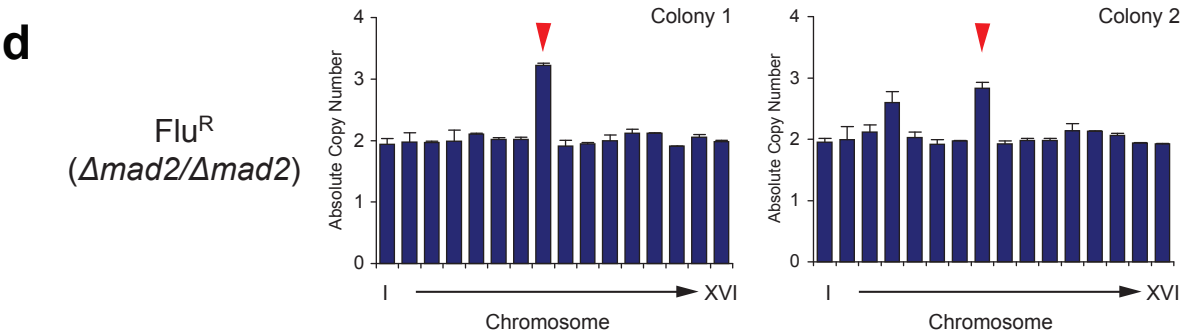
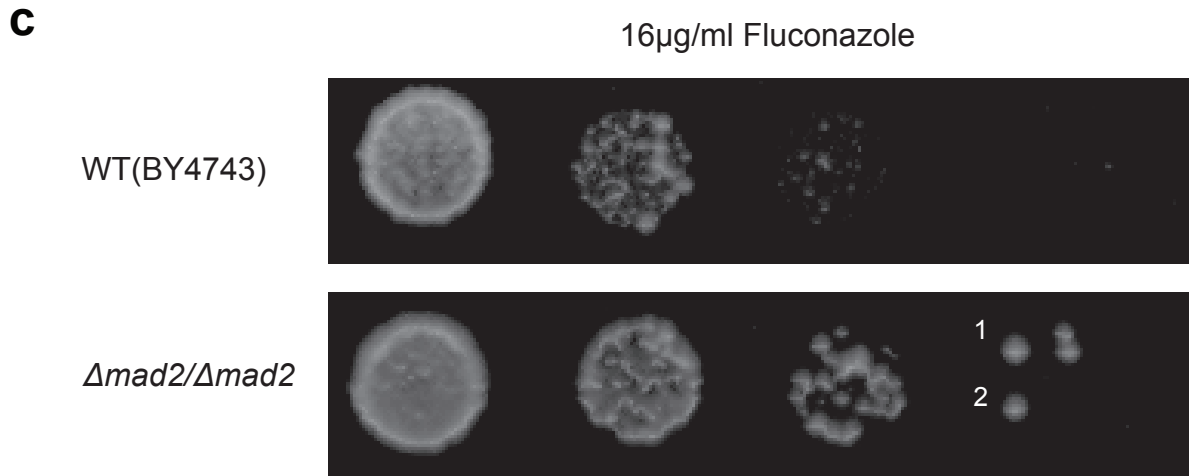
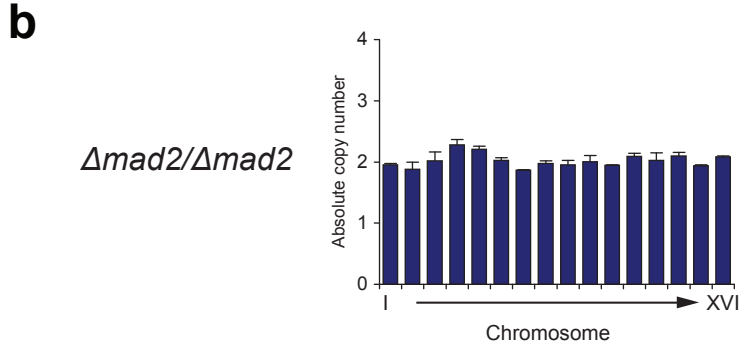
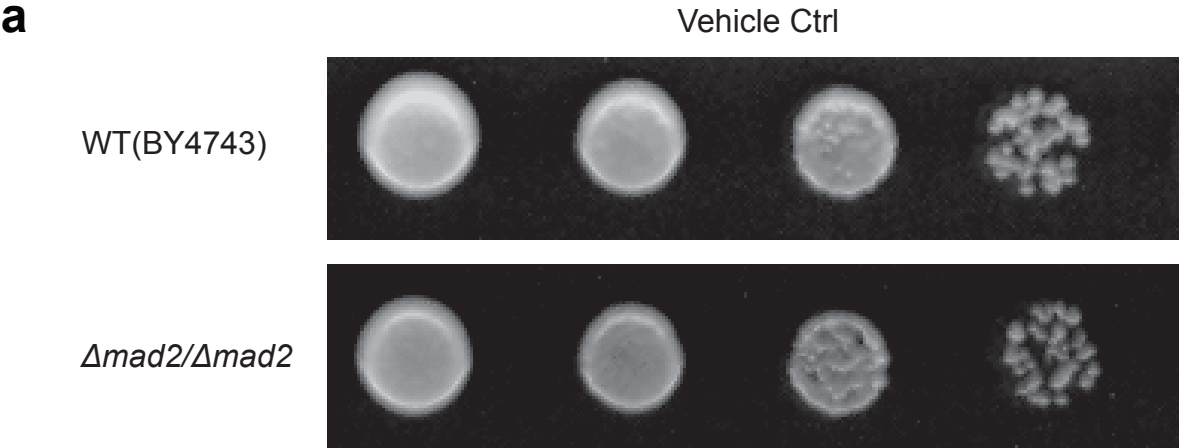
**c**



**d**



# Supplementary Figure 11



## Supplementary Figure Legends

### **Supplementary Figure 1. Summary: Hsp90 stress potentiates rapid cellular adaptation through induction of aneuploidy**

The study reveals that many stress conditions, especially Hsp90 inhibition, can elevate chromosomal instability in *Saccharomyces cerevisiae*. We also directly show that the stress-induced karyotype diversity, either by Hsp90 stress or by genetic perturbation (such as *MAD2* deletion), drastically potentiates the adaptation to environmental stress. During this process, the adaptive karyotype is selected and fixed within the population as long as the stress is present. If the environmental stress is attenuated, the population may return to euploidy. Spheres with varied colors and shapes represent cells with different karyotypes, which display phenotypic variation.

### **Supplementary Figure 2. Experimental Scheme for measuring CF loss rates induced by diverse stress conditions.**

**(a)** The structure of the artificial chromosome. ARS: autonomously replicating sequence. The gene suppressing the red pigment accumulation (*SUP11*) is located on the short arm, while the long arm is composed of an additional copy of Chr III left arm (Chr III.L). **(b)** Cells carrying CF, which give rise to white colonies, were grown in the presence of a specific chemical at two sub-lethal concentrations (low and high, Supplementary Fig. 3) for 14-16 hour and then plated onto stress-free rich media (YPD). The OD reading of the

liquid culture after incubation, total number of colonies on YPD plates and the number of red colonies, which lost CF, were recorded (Supplementary Fig. 3).

### **Supplementary Figure 3. Diverse stress conditions, especially Hsp90 inhibition, increase the red colony frequency.**

Top, the parameters of the colony color assay used to estimate the CF loss rate were reported. Bottom, red colony frequencies (number of red colonies over total colonies), were reported. Many stresses elevated CF loss rate. The CIN effect usually came along with strong inhibition of cell proliferation. However, radicicol, a Hsp90 inhibitor, led to a CF loss rate ~300x higher than the vehicle control and ~20x higher than benomyl, with only relatively minor growth inhibition. Data were normalized to vehicle-control. N.D.: no detection of red colony frequency increase over control.

### **Supplementary Figure 4. Hsp90 stress induces whole chromosome aneuploidy.**

(a) Both arms of artificial chromosome were lost in red cells induced by 10 $\mu$ g/ml radicicol treatment. The copy numbers of chromosome 3L, which is present on both endogenous Chr III and the chromosome fragment (CF), are shown in relative to Chromosome 3R. The red color of the colony suggested the loss of *SUP11*. The loss of both *SUP11* (on the CF short arm) and one copy of Chr 3L (the CF long arm) suggested that the whole CF artificial chromosome was lost in red colonies. Structure of CF is

presented in Supplementary Fig. 2a. Data were obtained with the qPCR assay. **(b, c)** Whole chromosome aneuploidy of other chromosomes was identified among the red colonies generated after the 10 $\mu$ g/ml radicicol treatment. **(b)** DNA flow-cytometry analysis of 13 different red colonies treated by radicicol is shown, in comparison with ones treated with vehicle control. No polyploidization was observed. **(c)** Comparative genomic hybridization results of a euploid control, colony 6 and colony 10 are presented with dots representing the probe intensity log<sub>2</sub>ratios over euploid. Repetitive elements were mapped to show regions where the copy number cannot be inferred from aCGH data <sup>21,22</sup>.

### **Supplementary Figure 5. Radicicol reduces Hsp90 function and impairs CBF3 complex assembly.**

**(a)**  $\Delta sti1$  showed higher sensitivity than  $\Delta hsp82$  to the presence of pharmacological inhibition of Hsp90. The maximum growth rate of wild type (WT),  $\Delta hsp82$  and  $\Delta sti1$  are shown. Bar graphs show mean $\pm$ SEM. n=4. **(b)** All but one components of CBF3 complex exhibited haploinsufficiency in the presence of radicicol. Sgt1 is the co-chaperone bridging the Hsp90-Sti1 complex to kinetochore <sup>23</sup>. Different strains were spotted at 10x serial dilutions from left to right. **(c)** Hsp90 stress disrupted the stoichiometry of kinetochore components. The localization of Ndc10-GFP and Cep3-GFP in different conditions is shown in a field larger than that in Figure 1c. Scale bar =2 $\mu$ m. **(d)** Quantification of the intensities of kinetochore GFP signals in anaphase cells under conditions as indicated. Bar graphs show mean $\pm$ SEM. n>20 cells/strain/condition. **(e)**

The percentages of cells with discrete kinetochore localization of Ndc10-GFP or Cep3-GFP were quantified. n>30 cells/strain/condition.

### **Supplementary Figure 6. Evolution experiment to select for stable radicicol resistant colonies**

Briefly, a diploid strain was first grown on plate containing high concentration of radicicol (100µg/ml) or vehicle control; three of the largest radicicol resistant colonies along with a colony from the vehicle plate were cultured overnight in drug-free media to wash out non-genetic effect and then retested for radicicol resistance (see Supplementary Methods for more details).

### **Supplementary Figure 7. Increased gene dosages of *ST11* and *PDR5* encoded on Chr XV are partially required and sufficient for conferring radicicol resistance.**

Representative growth curves for the indicated strains in 100 µg/ml radicicol are shown.

### **Supplementary Figure 8. Moderate and short-term Hsp90 inhibition drastically increases the karyotype diversity in the population.**

(a) Experimental scheme to test the effect of moderate and short-term Hsp90 inhibition on the adaptability of population to new stresses. A diploid culture was established from a single colony and split into two groups, which are pretreated for 2 days with either

vehicle control (V) or radicicol (R). They were then recovered in a drug-free environment for 24 hours to diminish non-genetic effects. The two groups were then plated on media containing 3 new stress-causing agents separately. The experiment was repeated three times. **(b, c)** The population after moderate and short-term Hsp90 inhibition showed drastically higher karyotype diversity. Immediately after the 2-day pre-treatment as mentioned above, the cell cultures treated by vehicle control (V group) or radicicol (R group) were plated onto YPD plates without drug. Single colonies were karyotyped by qPCR. **(b)** The karyotypes of 6 colonies from V group were characterized showing all 6 remained euploid. **(c)** The karyotypes of 18 colonies from R group were characterized showing 6 of the 18 were aneuploid with different karyotypes. **(d, e)** The karyotype diversity induced in radicicol pre-treatment was partially maintained after the recovery phase. The cell cultures pre-treated by vehicle control (V group) or radicicol (R group) were plated onto YPD plates with vehicle control after the recovery phase. **(d)** The karyotypes of 9 colonies from V group on vehicle control plates were characterized showing maintenance of euploidy. **(e)** The karyotypes of 21 colonies from R group on vehicle control plates are shown. Compared with Supplementary Fig. 8c, the karyotype diversity was reduced. This is likely attributed to the competition between cells bearing different karyotypes during the recovery phase. All karyotypes in this figure were determined by the qPCR assay.



### **Supplementary Figure 9. Independent drug-resistant colonies formed in the same new environment tend to share the same karyotype**

Resistant colonies formed in the same stress tend to be clustered together by their karyotype. Two major clusters, containing resistant colonies to tunicamycin and benomyl, respectively, are highlighted by bars. The hierarchical clustering was performed in R using the complete linkage method using the Euclidean distances.

### **Supplementary Figure 10. Chr XVI monosomy is unstable in stress-free environment and produces large (diploid) and small (Chr XVI monosomy) colonies**

**(a)** Colony size variation is due to karyotype instability of Chr XVI monosomy. Shown here are karyotypes of the Parent B and the progeny colonies B1-3 as determined by qPCR karyotyping. Sizes of these colonies on YPD plates are noted. See Figure 4 for similar result on Parent A lineage. Parent A and B are direct progenies of the colony V-Tun-1a and 1b, respectively, in Figure 3. **(b)** Only Chr XVI monosomy progenies but not euploid progenies retain tunicamycin resistance. Same numbers of cells were plated onto control and tunicamycin plates. **(c, d)** Growth curves of the euploid progenies (A3 and B3) and the ChrXVI monosomy progenies (A1 and B1) in YPD liquid media containing vehicle **(c)** or 2.5 µg/ml tunicamycin **(d)** are shown.

## Supplementary Figure 11. *MAD2* deletion can lead to adaptation to fluconazole through Chr VIII aneuploidy

(a, c) Diploid wild-type (BY4743) and  $\Delta mad2/\Delta mad2$  cells were spotted in 10-fold serial dilutions onto a YPD plate with either 1% DMSO (a) or 16 $\mu$ g/ml fluconazole (c), with the left most spot in each row containing around 200,000 cells. The plates were incubated for 36 hours at 30 °C. (b) qPCR karyotyping of  $\Delta mad2/\Delta mad2$  population grown on YPD showed that most  $\Delta mad2/\Delta mad2$  cells were euploid. (d) qPCR karyotyping showed that two  $\Delta mad2/\Delta mad2$  colonies well adapted to 16 $\mu$ g/ml fluconazole (Flu<sup>R</sup>, marked 1 and 2 in (c)) were aneuploid with an extra copy of Chr VIII (red arrows), which carries the *ERG11* gene, target of fluconazole. The increased dosage of this gene is known to confer fluconazole resistance in clinical isolates of *Candida albicans*<sup>24</sup>.

## Supplementary Methods

### Plasmids

Primers used are listed in Supplementary Table 3. pRLB473, a pRS305 based plasmid, was constructed to integrate an additional copy of *STII* into the original locus and it was cloned as follows. Primers Cp073 and Cp074 were used to amplify a fragment of DNA by PCR from budding yeast genomic DNA, containing the *STII* ORF and upstream/downstream sequences. This fragment was further amplified by using primers Cp078 and Cp079 to add a Not I cutting site to 5' and a Xho I to 3'. After restriction enzyme digestion, the fragment was inserted into pRS305. pRLB474, a pRS303 based plasmid, was constructed to integrate an additional copy of *PDR5* into the original locus. Primers Cp057 and Cp058 were used to PCR-amplify a fragment of DNA from budding yeast genome, containing the *PDR5* ORF and upstream/downstream sequences. This fragment was further amplified by Cp059 and Cp060 to add Not I to 5' and Xho I to 3', and inserted into pRS303. The above plasmids were sequenced to verify the absence of mutations in the ORF, by using primers Cs10-Cs18 and Cs21-Cs23.

### Media

YPD media were made by mixing 10g Bacto-yeast extract (#212720), 20g Bacto-peptone (#211830), 20g Bacto-agar (#214010) together with 950ml water, autoclaved and adding 50ml 40% glucose. After cooled to 60-65 °C, YPD was supplemented with 1% (v/v) DMSO or drugs dissolved in DMSO, and the plates were poured.

### *Saccharomyces cerevisiae* strains

The list of yeast strains is provided in Supplementary Table 2. Standard techniques were used for yeast transformations. *STII* and *PDR5* were deleted in Chr XV trisomy strain as follows. RLY6673, the Rad<sup>r</sup> 3 in radicol adaptation experiment with gain of only Chr XV, was streaked out from glycerol stock and karyotype-confirmed by qPCR. To delete one copy of *STII*, Cp027 and Cp028 were used to amplify the *HPH* gene, a hygromycin resistance marker, from a pFA6a backbone plasmid. A DNA fragment with the marker and 45bp homologous sequences flanking the upstream and downstream of *STII* was thus generated. RLY6673 was transformed with this fragment to generate RLY7011 where one copy of *STII* was deleted by homologous recombination. To delete one copy of *PDR5*, Cp065 and CP066 were used following the same procedure as described above for *STII* deletion. All deletions were verified by genomic PCR. As a previous report suggests transformation itself may induce aneuploidy<sup>25</sup>, the karyotypes of the transformants were reconfirmed by qPCR karyotyping assay, and the ones retaining the original karyotype (Chr XV trisomy) were selected.

To integrate one copy of *STII* into a haploid genome, RLB473 was linearized at BglII site and used to transform RLY2626. RLY2626 is a meiotic progeny with the *a* mating type of the diploid strain RLY2628 used in radicol adaptation experiment. The integration of one copy *STII* was verified by qPCR of genomic DNA using primers Cp088 and Cp089, yielding RLY7111. To integrate one copy of *PDR5* into RLY2627, a meiotic progeny with the *α* mating type of diploid RLY2628, RLB473 was linearized at Sall site before transformation. The integration of one copy *PDR5* was verified by DNA qPCR using primers Cp090 and Cp091, yielding RLY7114. RLY7111 was then crossed with RLY2627 to generate RLY7147, an *a/α* diploid strain with one additional copy of

*STII*. RLY7114 was crossed with RLY2626 to generate RLY7149, an a/α diploid strain with one additional copy of *PDR5*. RLY7111 was crossed with RLY7114 to construct RLY7148, an a/α diploid strain with one additional copy of both *STII* and *PDR5*.

### **Colony color assay for detecting CF loss induced by diverse stresses**

The CF is mostly a fragment of yeast Chr III, containing the left arm, the centromere, telomeres, and autonomous replication sequences (Supplementary Fig. 2a)<sup>26</sup>. It also contains *SUP11* and *URA3* marker on the right short arm. The transmission fidelity of the artificial chromosome was monitored by colony color. The background haploid strain carries an ochre *ade2* mutation, *ade2-101*, and confers a red colony phenotype. This red pigment accumulation can be suppressed by *SUP11*, carried on the CF, generating a white colony phenotype. Chromosome loss events are manifested by the appearance of red colonies<sup>27,28</sup>.

White colonies with CF (RLY4029) from YPD plates were used to inoculate overnight cultures in the -ura synthetic complete (SC) media grown 30°C. The culture was then diluted to OD<sub>600</sub> 0.1 in SC-ura media and grown for 6 more hours. The cells were then transferred to YPD media at the initial OD<sub>600</sub> of 0.2 containing either vehicle control (1% DMSO) or different stress reagents (Supplementary Table 1). The cultures were incubated for 14-16 hours at 30°C and final OD was recorded. Yeast cells were diluted to an appropriate density (determined in pilot experiments) and plated onto YPD plates. After 3 days of incubation at 30°C, the plates were moved to cold room (4°C) to allow accumulation of red pigment for easy visualization. Total and red colony number

were recorded. Due to the large number of plates, this experiment was performed in two batches with data combined.

### **Estimating chromosome loss rate ( $\gamma$ ) from red colony frequency ( $\alpha$ )**

In order to estimate the chromosome loss rate ( $\gamma$ ) per cell cycle, following parameters were measured:

b: The initial background frequency of rare cells giving rise to red colonies in -ura culture.

To determine b, white cells with CF were cultured in SC-ura overnight and directly plated onto YPD plates. In 19608 colonies counted, 12 colonies were found to be red, so the frequency of red cells in SC-ura culture was estimated to be 0.06%.

n: The number of cell cycle in the liquid YPD media containing stress inducing agents or vehicle.

n was estimated from OD reading, as

$$n = \log_2 \left( \frac{OD_{final}}{OD_{initial}} \right)$$

$\alpha$ : The red colony frequency, which represents the percentage of the red colonies on the YPD plates after the incubation with vehicle or stress-inducing agents.

$$\alpha = \frac{R_n}{R_n + W_n} = 1 - \frac{W_n}{T_n},$$

where,  $W_n$  = the number of white cells,  $R_n$  = The number of red cells, and  $T_n$  = The total number of cells, at generation n.

As  $W_x = (2 - \gamma)W_{x-1}$ , where  $\gamma$  = CF loss rate /division, it can be derived that

$$W_n = (2 - \gamma)^n W_0$$

Given  $T_n = 2^n T_0$ ,

$\alpha$  can be expressed as:

$$\begin{aligned}\alpha &= 1 - \frac{W_n}{T_n} = 1 - \frac{(2 - \gamma)^n W_0}{2^n T_0} \\ &= 1 - \left(1 - \frac{\gamma}{2}\right)^n \frac{W_0}{T_0}\end{aligned}$$

When  $\gamma \ll 1$ , the above expression can be approximated as:

$$\alpha \approx 1 - \left(1 - \frac{n\gamma}{2}\right) \frac{W_0}{T_0}$$

As the initial background frequency of rare red cells in SC-ura culture,  $b$ , can be expressed as:

$$\begin{aligned}b &= \frac{R_0}{T_0} = 1 - \frac{W_0}{T_0} \\ \Rightarrow \frac{W_0}{T_0} &= 1 - b\end{aligned}$$

and thus,

$$\alpha = 1 - \left(1 - \frac{n\gamma}{2}\right)(1 - b)$$

Resolving the above equation, the chromosome loss rate ( $\gamma$ ) can be expressed as:

$$\gamma = \frac{2(\alpha - b)}{n(1 - b)}$$

As  $b = 0.6 \times 10^{-3} \ll 1$ ,  $\gamma = \frac{2(\alpha - b)}{n}$

Using the above model, the loss rate of CF in YPD with vehicle control is computed to be  $2.1 \times 10^{-4}$ /division, similar to previous estimations based on sectoring assays<sup>29,30</sup>.

### **Colony color assay for detecting heat-shock induced CF loss**

RLY4029 (CF containing) cells cultured overnight in SC-ura media were transferred to YPD and OD adjusted to 0.5. 40 $\mu$ l aliquots of the resulting culture were transferred into PCR tubes and heat-shocked for 90s. The cultures were then cooled down to 23 °C. 600 untreated cells or 6,000 heat-shocked cells were plated onto YPD plates. More heat-shocked cells were plated due to the high lethality. After 3 days of incubation at 30°C, the plates were moved to cold room (4°C) to facilitate red pigment accumulation.

### **Imaging analysis of Ndc10-GFP and Cep3-GFP localization after radicicol treatment**

Yeast strains with C-terminal GFP tagging on *NDC10* or *CEP3* genes were retrieved from the GFP ORF tagging library<sup>31</sup>. All cultures were grown at 30 °C. Both strains were cultured overnight in SC media and dilute to OD 0.1 and further grown for 3 hours. The OD was again adjusted to 0.1 immediately prior to the addition of 1% Dimethyl sulfoxide (DMSO, vehicle control), 10  $\mu$ g/ml radicicol or 100  $\mu$ g/ml radicicol (final concentrations). After 4-6 hours incubations, Z-stack images were taken with an inverted Zeiss 200 m outfitted with a spinning-disc confocal system (Yokagawa) and an EM-CCD (Hamamatsu C9100), using a 100x oil objective lens.

To measure the intensity of the dot-like kinetochore localization of GFP signals, only large-budded anaphase cells with two distinct dots per cell were included, as prior to



anaphase, the kinetochore signal varies depending on the status of DNA replication. Extraction of data from images was performed by Image J software. The background was first subtracted. For cells within the central field of the image, a circle slightly larger than a normal dot was specified, where average fluorescence intensity was measured. The same circle was used for all measurements.

Since at 100µg/ml radicicol, a large proportion of cells failed to localize Cep3 to the kinetochore, cells were scored for the presence of the Cep3-GFP or Ndc10-GFP kinetochore localization to distinguish cells with discrete dot-like GFP localization on kinetochore from the ones with diffuse localization.

### **Selection for radicicol resistant yeast colonies**

~600 diploid RLY2628 cells were plated onto plates containing 100 µg/ml radicicol (1st drug plate) while 10 fold fewer (~60) RLY2628 cells were plated onto plates with vehicle control. At this radicicol concentration the cell survival rate as measured by colony formation was ~7%. After 7 days incubation at 30 °C, 3 largest colonies from each plate were picked and cultured, for roughly 5 generations, in drug-free YPD media overnight until saturation. This step was designed to diminish adaptation through non-genetic changes. The cultures were then plated again at ~400 cells/plate onto YPD media with radicicol (2<sup>nd</sup> drug plate) to re-test their drug resistance. After 3 days incubation at 30 °C, the images were taken. One colony randomly picked from each of triplicate of the 2<sup>nd</sup> drug plate was subjected to comparative genomic hybridization (CGH).

### **Comparative Genomic Hybridization**

Array construction and hybridization were carried out as described previously<sup>32</sup>. The arrays consisted of 23.3k 70-mer custom oligonucleotides designed to tile the yeast genome with an average spacing of 528 bp. Genomic DNA was extracted using YeaStar™ Genomic DNA Kit (Zymoresearch), and then labeled for array analysis using the BioPrime Plus Array CGH Kit (Invitrogen). Data analysis was performed with the R programming language. Array intensities were background subtracted and normalized using the loess method from the limma package<sup>33</sup>. After global normalization, probe groups representing each chromosome were further adjusted by dividing each by the median of all chromosomes. The karyotype for each chromosome was determined by the median  $\log_2(\text{test strain/wt})$  for all probes representing that chromosome. For visualization, the data were then sorted by chromosomal position and smoothed using a running median with a window size of 7 probes.

### **Quantitative growth Assays**

The quantitative growth assays were performed with a previously reported protocol<sup>34</sup>. Cells were cultured to saturation in YPD or SC-His+100 $\mu\text{g/ml}$  G418 (used for genetically constructed Chr XV disomy and the control euploid strains<sup>35</sup>) and then were dilute 100 times into YPD with either vehicle control or drug (such as radicicol or tunicamycin)-containing media and split into 4 independent cultures as replicates. The 96-well or 48-well plate (Falcon) was filled with 100 $\mu\text{l}$  liquid and sealed with parafilm. The optical density (OD) at 595nm was continuously monitored at 30 °C using a Tecan Infinite M200 Pro. The data were extracted and analyzed by Magellan 7 software. For growth assay on strains with a known aneuploidy karyotype, each strain was streaked into

single colonies and karyotyped again right before growth assay to make sure that the tested strains retained the original karyotype.

### **Determination of karyotype diversity caused by short-term radicicol treatment**

All incubations were performed at 30 °C. RLY6864, a diploid strain in the same background as the CF strain was cultured in YPD overnight to reach saturation, diluted in fresh YPD and grown to OD 0.5. The cultures were then diluted to OD 0.05 in YPD media with 20µg/ml radicicol or vehicle control (1% DMSO). After 24 hours, the culture reached saturation and was diluted 100x and cultured further. The next day, the cultures were plated on YPD plates without drug to form single colonies, which were karyotyped by DNA qPCR.

### **Flow cytometry analysis of DNA content**

A protocol optimized from that previously reported<sup>36</sup> was used to process yeast cells for DNA analysis by flow cytometry with improved ploidy resolution and throughput. As the purpose of this analysis was to identify changes in ploidy, cells were grown to saturation (which led to a high and discrete G1 peak in Supplementary Figure 4b). The cells were harvested, washed once with water, and fixed in 70% ethanol in a 96-well plate for 1 hour. Samples were then transferred into a 96-well polypropylene filter (Whatman), where the ethanol was removed by vacuum and the cells washed twice with water. 100 µl 2mg/ml RNase (Sigma) solution was then added to remove the RNA. After 2 hour incubation, 5mg/ml trypsin (Sigma) was added to digest the protein thoroughly. This procedure continued overnight at 37 °C and was the key for much improved DNA

peak resolution over previous protocols. The cells were then washed in 50mM Tris 7.5 buffer and sonicated. 2 $\mu$ M Sytox Green dye (Invitrogen) was added to stain the DNA. The data was collected with the FITC channel on an Influx cytometer (BD Biosciences), and analyzed by Flowjo.

### **Karyotyping yeast cells by DNA qPCR**

The detailed protocol used to karyotype yeast cells by DNA qPCR has been described elsewhere<sup>37</sup>. Briefly, a pair of qPCR primers was designed for each of the 2 pericentromeric regions flanking every centromere. By measuring the relative copy number of these pericentromeric DNA fragments through DNA qPCR in comparison to a known euploid strain, the number of each chromosome was determined.

### **Testing the adaptability of the population with karyotype diversity induced by Hsp90 stress**

The initial pre-treatment process was essentially the same as described in the short-term radicicol treatment. Three lines of independent cultures were established, each from a single colony and split into two groups: one with 20 $\mu$ g/ml radicicol, the other with 1% DMSO control. After the karyotype diversity was generated, each line of culture was washed with YPD 3 times and then diluted 100x in YPD without any drug. This recovery step lasted for 24 hours to recover from any non-genetic effects caused by radicicol pre-treatment. The cells were then plated either at 40,000 cells/plate onto new stress plates or at 40 cells/plate onto control YPD plates with 1% DMSO. The plates were incubated at 30 °C for around 7 days.

The plates were imaged by using a scanner (HP Scanjet 4070) and colony number and sizes recorded using an automatic colony identification software - imageQuantTL. All the colonies formed under the same stress conditions were ranked according to their sizes.

### **Assays to test the linkage between Chr XVI monosomy and tunicamycin resistance**

Strain V-Tun-1a and V-Tun-1b were streaked out from glycerol stock into single colonies. From passage 1, one small colonies of each strain were karyotyped by qPCR and patched on YPD plates so that high density of cell colonies can form to enrich the rare big colonies. The patches were further streaked out to single colonies.

Single colonies with different sizes were karyotyped by qPCR. Colony growth was characterized right after karyotyping by both colony formation on solid plates and growth curve in liquid media. For colony formation assay, a portion of the fresh colonies were directly plated onto YPD plates with vehicle control or 2.5 $\mu$ g/ml tunicamycin at the same density of ~50 cells/plate. The plates were incubated in 30 °C for around 7 days before images were taken. Meanwhile, a small portion of colonies were cultured in YPD to saturation, karyotyped by qPCR again and then diluted 100x into YPD with either vehicle control or 2.5 $\mu$ g/ml tunicamycin. 4 replicates of each colony from each condition were monitored for the growth by using a Tecan Infinite M200 Pro reader, as described above.

## Reference

- <sup>21</sup> Rancati, G. *et al.* Aneuploidy Underlies Rapid Adaptive Evolution of Yeast Cells Deprived of a Conserved Cytokinesis Motor. *Cell* **135**, 879-893, doi:10.1016/j.cell.2008.09.039 (2008).
- <sup>22</sup> Pinkel, D. & Albertson, D. G. Comparative genome hybridization. *Annual Review of Genomics and Human Genetics* **6**, 331-354, doi:10.1146/annurev.genom.6.080604.162140 (2005).
- <sup>23</sup> Catlett, M. G. & Kaplan, K. B. Sgt1p Is a Unique Co-chaperone That Acts as a Client Adaptor to Link Hsp90 to Skp1p. *Journal of Biological Chemistry* **281**, 33739-33748 (2006).
- <sup>24</sup> Selmecki, A., Gerami-Nejad, M., Paulson, C., Forche, A. & Berman, J. An isochromosome confers drug resistance in vivo by amplification of two genes, ERG11 and TAC1. *Molecular Microbiology* **68**, 624-641, doi:10.1111/j.1365-2958.2008.06176.x (2008).
- <sup>25</sup> Bouchonville, K., Forche, A., Tang, K. E. S., Selmecki, A. & Berman, J. Aneuploid Chromosomes Are Highly Unstable during DNA Transformation of *Candida albicans*. *Eukaryotic Cell* **8**, 1554-1566 (2009).
- <sup>26</sup> Spencer, F., Gerring, S. L., Connelly, C. & Hieter, P. Mitotic Chromosome Transmission Fidelity Mutants in *Saccharomyces cerevisiae*. *Genetics* **124**, 237-249 (1990).

- 27 Yuen, K. W. Y. *et al.* Systematic genome instability screens in yeast and their potential relevance to cancer. *Proceedings of the National Academy of Sciences* **104**, 3925-3930, doi:10.1073/pnas.0610642104 (2007).
- 28 Hieter, P., Mann, C., Snyder, M. & Davis, R. W. Mitotic stability of yeast chromosomes: A colony color assay that measures nondisjunction and chromosome loss. *Cell* **40**, 381-392 (1985).
- 29 Gerring, S. L., Spencer, F. & Hieter, P. The CHL 1 (CTF 1) gene product of *Saccharomyces cerevisiae* is important for chromosome transmission and normal cell cycle progression in G2/M. *EMBO J* **9**, 4347-4358 (1990).
- 30 Shero, J. H. *et al.* Analysis of chromosome segregation in *Saccharomyces cerevisiae*. *Methods in Enzymology*, 749-773 (1991).
- 31 Huh, W.-K. *et al.* Global analysis of protein localization in budding yeast. *Nature* **425**, 686-691 (2003).
- 32 Sinibaldi, R., O'Connell, C., Seidel, C. & Rodriguez, H. Gene expression analysis on medium-density oligonucleotide arrays. *Methods Mol Biol* **170**, 211-222, doi:10.1385/1-59259-234-1:211 [doi] (2001).
- 33 Smyth, G. K. Linear models and empirical bayes methods for assessing differential expression in microarray experiments. *Stat Appl Genet Mol Biol* **3**, Article3, doi:10.2202/1544-6115.1027 [doi] (2004).
- 34 Toussaint, M. & Conconi, A. High-throughput and sensitive assay to measure yeast cell growth: a bench protocol for testing genotoxic agents. *Nat. Protocols* **1**, 1922-1928 (2006).

- <sup>35</sup> Torres, E. M. *et al.* Effects of Aneuploidy on Cellular Physiology and Cell Division in Haploid Yeast. *Science* **317**, 916-924, doi:10.1126/science.1142210 (2007).
- <sup>36</sup> Haase, S. B. & Reed, S. I. Improved Flow Cytometric Analysis of the Budding Yeast Cell Cycle. *Cell Cycle* **1**, 117-121 (2002).
- <sup>37</sup> Pavelka, N. *et al.* Aneuploidy confers quantitative proteome changes and phenotypic variation in budding yeast. *Nature* **468**, 321-325 (2010).



## Supplementary Table 1: Chemicals used to cause stresses

Chemical Name	Type of Stress	Drug Target	Source
Hydrogen peroxide	oxidative stress		
Sodium chloride	osmotic stress		Sigma
Tunicamycin (Tun)	Protein glycosylation; ER stress	GlcNAc phosphotransferase (ALG7)	Sigma
Benomyl (Ben)	Spindle assembly	tubulin	Sigma
Amphotericin B (Amph)	Membrane integrity defect		Sigma
Fluconazole (FL)	Membrane integrity defect; ergosterol synthesis impaired	14 $\alpha$ -demethylase (ERG11)	Sigma
Cycloheximide (Cyc)	Protein synthesis	ribosome	Sigma
4-Nitroquinoline 1-oxide (4NQO)	Replicative stress caused by base alkanoylation		Sigma
Radicicol (Rad)	Proteotoxic; Hsp90	<i>Hsp82; Hsc82</i>	AG Scientific
Macbecin II	Proteotoxic; Hsp90	<i>Hsp82; Hsc82</i>	DTP, Nat. Cancer Institute

## Supplementary Table 2: Yeast strains used in the paper

Name	Background	Description	Source
RLY-2626	S288C	MAT $\alpha$ ; ura3-52; his3- $\Delta$ 200; trp1-1; leu2-3	(14)
RLY-2627	S288C	MAT $\alpha$ ; ura3-52; his3- $\Delta$ 200; trp1-1; leu2-3	(14)
RLY-2628	S288C	2626x2627	(14)
RLY-4029	S288C	MAT $\alpha$ ; ura3-52; lys2-801; ade2-101; trp1D1; leu2D1; +CFIII(CEN3.L.YFS2.1)URA3; SUP11; leu2D1	gift from Dr. F. Spencer
RLY-4774	S288C	As RLY-4029; $\Delta$ hsp82::KAN	This study
RLY-4777	S288C	As RLY-4029; $\Delta$ sti1::HPH	This study
RLY-6673	S288C	MAT $\alpha$ / $\alpha$ ; ura3/ura3; his3/his3; trp1/trp1; leu2/leu2; +Chr XV	This study
RLY-6864	S288C	MAT $\alpha$ / $\alpha$ ; ura/ura; lys/lys; ade2-101/ade2-101; leu/leu; HIS/his; trp/trp	This study
RLY-6933	W303	MAT $\alpha$ ; ade2-1; leu2-3; ura3; trp1-1; his3-11; 15; can1-100; ade1::HIS3; lys2::KanMX6; GAL; [psi+]	(11)
RLY-6945	W303	MAT $\alpha$ ; ade2-1; leu2-3; ura3; trp1-1; his3-11; 15; can1-100; leu9::HIS3; GAL; [psi+] +ChrXV leu9::KanMX6	(11)
RLY-7011	S288C	MAT $\alpha$ / $\alpha$ ; ura3/ura3; his3/his3; trp1/trp1; leu2/leu2; STII/STII; +Chr XV $\Delta$ sti1::HPH	This study
RLY-7012	S288C	MAT $\alpha$ / $\alpha$ ; ura3/ura3; his3/his3; trp1/trp1; leu2/leu2; PDR5/PDR5; +Chr XV $\Delta$ pdr5::HPH	This study
RLY-7111	S288C	MAT $\alpha$ ; ura3-52; his3- $\Delta$ 200; trp1-1; leu2-3; +STII( RLB473 integration, LEU)	This study
RLY-7114	S288C	MAT $\alpha$ ; ura3-52; his3- $\Delta$ 200; trp1-1; leu2-3; +PDR5 (RLB474 integ, HIS)	This study
RLY-7147	S288C	7111x2627	This study
RLY-7148	S288C	7111x7114	This study
RLY-7149	S288C	7114X2626	This study
RLY-7306	S288C	MAT $\alpha$ ; his3 $\Delta$ 1; leu2 $\Delta$ 0; met15 $\Delta$ 0; ura3 $\Delta$ 0; NDC10-GFP::HIS3MX6	(7)
RLY-7307	S288C	MAT $\alpha$ ; his3 $\Delta$ 1; leu2 $\Delta$ 0; met15 $\Delta$ 0; ura3 $\Delta$ 0; CEP3-GFP::HIS3MX6	(7)
RLY-7438	S288C	MAT $\alpha$ ; ura3-52; lys2-801; ade2-101; trp1D1; leu2D1	This study
RLY-7439	S288C	MAT $\alpha$ ; ura3-52; lys2-801; ade2-101; trp1D1; leu2D1	This study
RLY-7440	S288C	(N-Tun-1a) As RLY-6864; -ChrXVI	This study
RLY-7441	S288C	(N-Tun-1b) As RLY-6864; -ChrXVI	This study

### Supplementary Table 3: Primers used in the study

Name	Oligo Sequence
cp017-hsp82-kanmx4-A	GGACGCATAATGAAAGCAGA
cp018-hsp82-kanmx4-B	AAGCCTTGAGAGACTCTTCCA
cp019-hsp82-kanmx4-C	CGGTGTTGATGATCAAACCTCA
cp020-hsp82-kanmx4-D	CTTGCGTGTGCGTATTTGTA
cp025-pfa-antibiotic-B	CTGCAGCGAGGAGCCGTAAT
cp026-pfa-kan-C	TGATTTTGATGACGAGCGTAAT
cp027-sti1 del-F	ATTCCTCACTGTAGCTACTAAAACAACCTATACGCAAGAAAGATGCGTAC GCTGCAGGTCGAC
cp028-sti1 del-R	AAAAAAGAATTCAAGATAATAAAGTTATATTTTCGTATTATTTTAAATCGA TGAATTCGAGCTCG
cp029-sti1 del-A	CCAAACTATTGAACTAAACGCAAGT
cp030-sti1 del-B	ATGTAGCCATGATGGTCATTAATCT
cp031-sti1 del-C	TCCAAATTTTCGTGAGAGCTTATATC
cp032-sti1 del-D	TTTTTCGCATTCTGATGTAATGAATA
cp033-pfa-Hph-C	GTTGACGGCAATTTTCGATGAT
cp057-PDR5 genome PCR-F	ATGTCTTCCTCTTTGATTCCAA
cp058-PDR 5 genome PCR-R	TTCGTTGTA CTCCAGTCGTGA

cp059-PDR5 genome PCR to pRS30x-F NotI	ATAATAGCGGCCGCATGTCTTCCTCTTTGATTCCAA
cp060-PDR 5 to pRS30x-R xhoI	ATAATACTCGAGTTCGTTGTA CTTCAGTCGTGA
cp065-pdr5 deletion-F	TTAAGTTTTTCGTATCCGCTCGTTTCGAAAGACTTTAGACAAAAATGCGTAC GCTGCAGGTCGAC
cp066-pdr5 deletion-R	CATCTTGGTAAGTTTTCTTTCTTAACCAAATTCAAAATTCTATTAATCGAT GAATTCGAGCTCG
cp067-pdr5 deletion confirm-A	TTGAACGTAATCTGAGCAATACAAA
cp068-pdr5 deletion confirm-D	TCACACTAAATGCTGATGCCTATAA
cp073-STI1 5' genomic primer	AATGGCCTGATAGAGGTTATCGAC
cp074-STI1 3' genomic primer	AGAAATTCCTAGGGCTGATCC
cp077-STI1 5' genomic to pRS30x primer	ATAATAGCGGCCGCAATGGCCTGATAGAGGTT
cp078-STI1 3' genomic primer to pRS30x-xhoI	ATAATACTCGAGAGAAATTCCTAGGGC
cp088-STI1 qPCR	TGAAAGATCCTGAAGTGGCTGCGA
cp089-STI1 qPCR	TGATACCAGCAGCGATCAACGTCT
cp090-PDR5 qPCR	TGTTGGCTGTTGGTGTGCTAACG
cp091-PDR5 qPCR	ACATGTCATACCGGATGGTGGTGT
cs9-SqP for PDR5-yeast genome pcr product_01	ATAATAGAAAGCAGCACCTC
cs10-SqP for PDR5-yeast genome pcr product_02	TGGCTGTTTCGCTTTTATTAT

cs11-SqP for PDR5-yeast genome pcr product_03	AGAACTTAAGTGCTTCTGGT
cs12-SqP for PDR5-yeast genome pcr product_04	GGATAATGCTACAAGGGGTT
cs13-SqP for PDR5-yeast genome pcr product_05	ATGGCTTTAATCTTGGGTTC
cs14-SqP for PDR5-yeast genome pcr product_06	TGCAAACATTTCTAGTACAG
cs15-SqP for PDR5-yeast genome pcr product_07	CAATGGTATTCCCCGTGATA
cs16-SqP for PDR5-yeast genome pcr product_08	GGCTCTCATGCAAATCAAGA
cs17-SqP for PDR5-yeast genome pcr product_09	TCTACGTTTATGTTGGTTCT
cs18-SqP for PDR5-yeast genome pcr product_10	ATCACTACATATAGGTGCGT
cs21-SqP for sti1_1	TGGTATCATCCGGACTGGCC
cs22-SqP for sti1_2	GGGGTTGATTTAAACATGGATGAT
cs23-SqP for sti1_3	CCTGAAAAGGCGGAGGAAGC